Sensors & Actuators: A. Physical 369 (2024) 115102

Contents lists available at ScienceDirect

Sensors and Actuators: A. Physical

journal homepage: www.journals.elsevier.com/sensors-and-actuators-a-physical

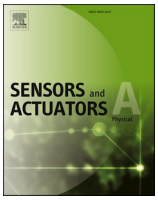

Design and development of a stretchable electronic textile and its application in a knee sleeve targeting wearable pain management

Meijing Liu [a,b,*], Gillian Lake-Thompson [b], Alison Wescott [b], Steve Beeby [a], John Tudor [a], Kai Yang [b]

[a] School of Electronics and Computer Science, University of Southampton, Southampton, UK
[b] Winchester School of Art, University of Southampton, Southampton, UK

ARTICLE INFO

Keywords:
Stretchable electronic textile
Lamination
Wearable technology
Stretchability measurement
Durability testing
Garment design

ABSTRACT

This paper presents the development of a stretchable electronic textile (e-textile) and the design of a knee sleeve with integrated electrodes for wearable applications. The e-textile is achieved by laminating a printed conductive pattern onto knitted fabric, followed by printing a carbon rubber electrode layer on top of the conductive pads of the conductive pattern. The Young's modulus of two knitted stretchable fabrics, made of different textile yarns, is tested and their impact on the e-textile and garment properties is discussed. Four printed conductive track designs in the form of a straight line, a sine wave, a half circle, and a horseshoe are laminated on these fabrics. The four designs are investigated in terms of conductivity, change during stretching, relaxation after stretching, and wash durability. A snap connector, attached to each end of the conductive tracks, provides electronic interconnection. The e-textiles survive 100 wash cycles with a resultant maximum resistance increase of 1.44 times. A fitted knee sleeve, for use in wearable electrotherapy for knee joint pain management, is fabricated by laminating a conductive track in the optimal sinusoidal design and then printing carbon rubber electrodes on top.

1. Introduction

Electronic textiles (e-textiles) are advanced textiles with integrated electronic functionality [1] ranging from conductive interconnection [2], sensing/actuating [3], signal processing [4,5] and wireless communication [6,7]. Advanced e-textile technologies offer a platform to realise wearable healthcare devices of which the market is projected to reach $168.2 billion by 2030 from $26.8 billion in 2022 [8]. Textiles are soft, breathable, and comfortable to wear. Making e-textiles into a garment (e.g. vest, sleeve) provides a convenient solution for healthcare monitoring and treatment which improves the user experience and increases user compliance, thus improving quality of life and reducing healthcare costs.

Our previous work has demonstrated skin interfaced e-textile applications in biopotential monitoring [9], stroke rehabilitation [10] and pain management [11]. These e-textiles incorporated conductive tracks and electrodes which are fundamental elements used to either perform electrocardiography (ECG) or electromyography (EMG), or, in the case of therapeutic devices, to deliver electrical impulses to the skin to exercise/strengthen muscles and reduce pain. Previously, the electrodes were printed on non-stretchable fabrics and made into wearable devices by attaching the printed fabrics to a wearable item (e.g. a knee sleeve) that can be worn on the body; this facilitated close contact between the electrodes and the skin even during movement. This approach, based on attaching a non-stretchable printed e-textile to a wearable item, increases the total thickness of the wearable, reduces flexibility and breathability, and negatively affects the aesthetic appearance. In order to overcome these limitations, it is essential to develop a thin, flexible, stretchable and durable e-textile which can be made into a wearable device.

Stretchable e-textiles are primarily made using knitting which is a well-established technique in the textile industry to realise stretchable, high elasticity fabrics. Knitting is used in various e-textile applications such as smart socks [12], gloves [13] and vests [14]. In such wearable functional e-textiles, the connection of the conductive yarn to the electrical wire is challenging, often exhibits low durability, and is unreliable. In this paper, instead of using an electrical clip [13] or wrapping the connection point using tape [14], a metal snap button is assembled on the knitted fabric to provide interconnection, offering a reliable and simple connection to external electronics.

* Corresponding author at: School of Electronics and Computer Science, University of Southampton, Southampton, UK.
E-mail address: MeijingLiu@soton.ac.uk (M. Liu).

https://doi.org/10.1016/j.sna.2024.115102
Received 30 October 2023; Received in revised form 15 January 2024; Accepted 31 January 2024
Available online 3 February 2024

An alternative method to knitting to achieve an e-textile is to print or laminate conductive tracks directly on the stretchable fabric. For example, Ke et al. [15] printed silver nanowires on fabric to achieve stretchable electronics. Wearable sensors [16,17] and illuminated clothing [18] can also be achieved using the printing/laminating approach. Printed conductive tracks on stretchable fabrics tend to be more easily damaged than laminated tracks as the printed materials are absorbed into the gaps between fabric yarns [15]. Furthermore, the laminated tracks are printed on a smooth plastic surface resulting in a more uniform structure than when printing directly on a rough textile. In the lamination approach, an adhesive layer on the back of the smooth plastic surface improves the adhesion to fabrics compared to direct printing. This paper evaluates the performance of laminated conductive tracks on a stretchable knitted fabric and discusses how to achieve optimal performance.

In all approaches, the wearable must have sufficient reliability and durability for the application. The textile and conductive component's properties and the level of strain to which they are subject in the application affects the reliability and durability of the e-textile. As an example, 50% strain occurs in the material stretched over the knee joint resulting from rotation during exercise [19,20]. This must be addressed in durability testing. The evaluated prototype in this paper is designed for knee osteoarthritis patients to relieve pain during exercise. The garment, including conductive tracks, aims to survive 50% strain, provide wash ability and prevent the prototype moving due to body movement.

This paper investigates two types of elastic fabric with four geometries of laminated conductive film. Section 2 describes the materials, and the methods of fabrication and testing. Section 3 presents the properties of the e-textiles in terms of their Young's modulus, strain relaxation after stretching, conductivity during stretching and recovery, and wash durability. Section 4 describes a prototype design for wearable electrotherapy application. Section 5 presents conclusions.

2. Experimental details

2.1. Textiles

The two types of textiles used in this study were supplied by Best Pacific Limited (Dongguan, China). AEI80580S5-B12 (called 'blue fabric' in this study) is a blue knitted double bed jersey fabric with a fibre composition of 53% acrylic, 27% modal, 4% silk, 5% cupro, and 11% Lycra. It is soft, water absorbent, and breathable. BEI81381MFX2 (called 'grey fabric' in this study) is a knitted grey fabric composed of 32% Lycra, 34% polyester, and 34% polyamide, which is also double bed jersey structure. The grey fabric exhibits higher elasticity and mechanical strength, but a coarser texture. Both fabrics are stretchable and therefore can be used to make tight-fitting clothing; these fabrics have also been pre-tested and shown to be compatible with the electrode and conductive track materials and the lamination process.

2.2. Conductive film and lamination

Conductive films with different track patterns were printed using transfer technologies developed at Conductive Transfers Limited (Barnsley, UK). A conductive transfer film is made by screen printing functional materials in the sequence of: 30 μm thick encapsulation insulating ink, 12 μm thick conductive ink, 30 μm thick insulating ink, and 70 μm thick adhesive ink. Each layer is shown in Fig. 1(a). The thickness of the plastic film is 120 μm. The size of the conductive films is specified in Section 2.4. As shown in Figure (b), the conductive layer is sandwiched between two insulating layers but with some of the conductive layer being selectively exposed by the patterned insulating layer in order to allow electrical connection at each end of the conductive track. By inverting the conductive film as shown in Fig. 1(c), the top adhesive is contact with fabrics and allows the conductive layer to adhere to the textile in the lamination process. .

The process of attaching the printed layers on the plastic film to the textile uses a heat press (Geo Knight DK20S) at a temperature of 165 °C [22,23]. The fabric is positioned on the heat press bed and the transfer is placed over the fabric with the printed pattern face down to ensure direct contact between the adhesive layer and the textile. A piece of lamination paper is placed over the transfer to stop the plastic film from sticking to the heat plate head. The press is closed compressing the transfer onto the textile for 20 s at 6 bar pressure. The pressed transfer and textile is removed from the press and allowed to cool for a minimum of 10 s and then the plastic film is peeled off. To improve the adhesion between the textile and the conductive layer, the laminated conductive fabric is then further heat pressed for an additional 6 s at 6 bar.

2.3. Snap button connector

A snap connector was assembled on the conductive fabric to allow interconnection with external electronics. Table 1 shows the structure of the traditional snap button used, consisting of a female part and a male part. The cap and socket combine to form the female part; the stud and post contribute to the male part. The female part has been integrated into commercially available TENS cables [24]. The stud and post clamp the e-textile in between them.

The snap connector is fabricated by placing the exposed conductive layer, located at the end of the conductive tracks on the conductive fabric, between the stud and the post of the snap button (Fig. 3). First, a hole is punched into the conductive layer to provide electrical connection between the stud and post. A press (Fig. 3(f)) is then used to apply pressure, enabling a uniform and reliable connection between the stud, post, and conductive layer.

As the snap connector is a component assembled from different constituent parts, it is positioned in a low-stretch area of the sleeve to minimise any potential damage caused by stretching which may lead to the disassembly of its constituent parts. The chosen area should also be easy for the user to reach to connect/disconnect the device when worn on the body. In this work, the connector is located on the outside of the knee as shown in Fig. 13(d).

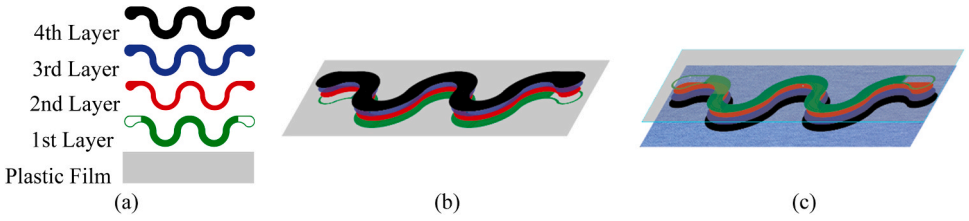

Fig. 1. : Schematic of the layers in a conductive film. (a) from the bottom to the top, these are the plastic film substrate, the encapsulation insulating ink, the conductive ink, the insulating ink, and the adhesive ink; (b) the front view of a conductive film made of the four layers in Fig. 1(a); (c) the conductive film is inverted from Fig. 1(b) and placed on a blue fabric before lamination.

Fig. 2. The schematic diagram of the lamination process. (a) step1: preparing the conductive films and fabric. (b) step 2: placing the conducive films on the fabric with the adhesive layer face down before heat pressing using a Geo Knight DK20S press [21]. (c) step 3: cooling down the sample and peeling off the plastic films.

Table 1
Components of the snap button [25] and the structure of a snap connector.

Part	Name	Snap button	Connector
Female	Cap Socket	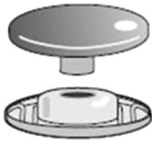	
Male	Stud Post	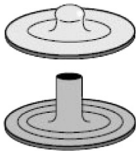	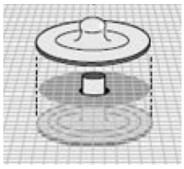

2.4. Design of the conductive tracks

A variety of interconnect structure configurations, including sine wave [26], half circle [27] and horseshoe shape [28], have been evaluated for their impact on stretchability.

In this study, the four shapes were designed with a vertical distance of 10 cm and a track width of 5 mm (Fig. 4). The amplitude of the sine wave and the radius of the half circle and the horseshoe are set to 12.5 mm. The horseshoe shape consists of repeated 240 degrees arcs [29]. The length of the conductive tracks for the straight line, sine wave, half circle and horseshoe are 10 cm, 14.64 cm, 15.71 cm and 26.18 cm respectively.

Every fabric test sample is cut to 6 cm wide and 17 cm long. The samples are 6 mm in thickness. Fig. 5 shows the conductive film on both the blue and grey fabrics.

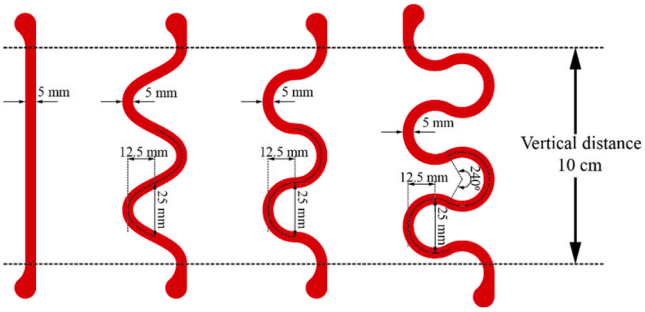

Fig. 4. : The 4 types of interconnect structure: straight, sine wave, half circle and horseshoe, from left to right.

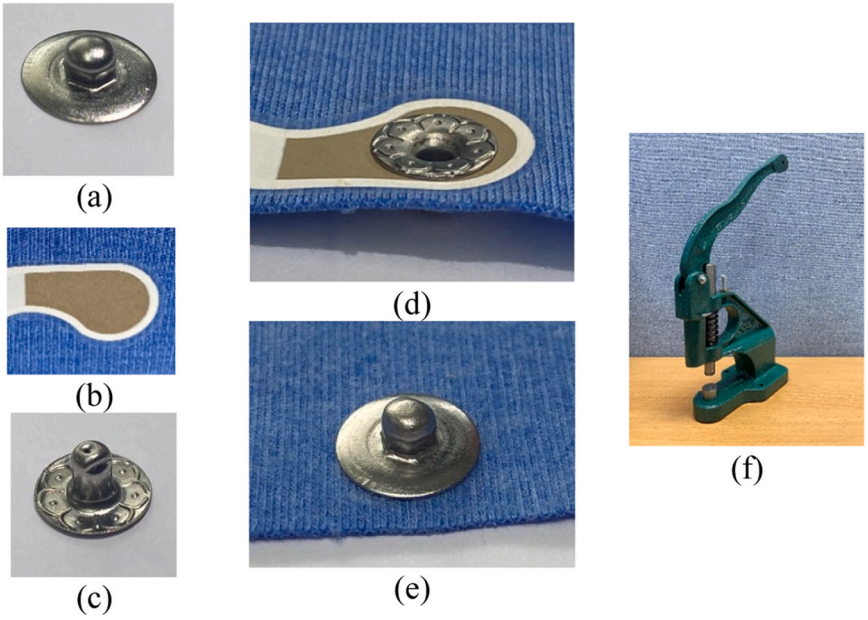

Fig. 3. (a) the stud part of the male connector, (b) blue fabric with laminated conductive layer (white: insulator, brown: conductor), (c) the post part of the male connector, (d) the conductive track with the post part of the connector fitted, (e) the stud fitted to the post of the male connector, (f) press machine with accessories pin.

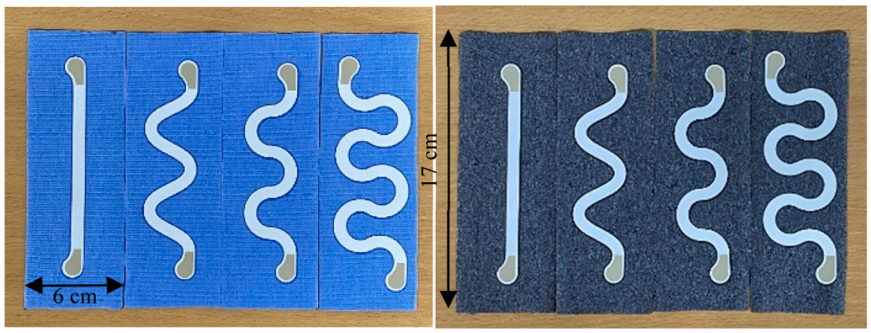

Fig. 5. : The 4 track designs laminated on both the blue and grey fabrics.

2.5. Test methods

2.5.1. Young's modulus of the fabrics

Young's modulus provides a measure of the force required to produce a textile extension. It is defined as the ratio of stress to strain.

$$\text{Young's modulus}(E) = \frac{\text{Stress}\quad(\sigma)}{\text{Strain}(\varepsilon)}$$

Where stress is the amount of force applied per unit area and strain is extension per unit length.

$$\text{Stress}\quad(\sigma) = \frac{\textit{Tensile force}(F)}{\textit{Fabric cross area}(A)} = \frac{\textit{Tensile force}(F)}{\textit{Fabric width}(W)\times\textit{Fabric thickness}(H)}$$

$$\text{Strain}(\varepsilon) = \frac{\textit{Extended length}(L)-\textit{Initial length}(L_0)}{\textit{Initial length}(L_0)}$$

A Tinius Olsen H25KS tensometer is used in this study. The tensile force (F) and extended length (L) are recorded during stretching, and stress-strain plots are generated by the tensometer.

2.5.2. The effect of stretch on e-textile resistance

Understanding the conductive track's electrical properties under stretch is essential for application in wearable technology for prototype design, application and power consumption. This test aims to measure the impact of fabric extension on the resistance of the conductive track. Fig. 6(a) shows the apparatus which was built for this research. It contains two clamps installed on a base with an adjustable distance between them. Insulating films are applied between the metal clamps and the conductive silver pads. The sample is clamped at 10 cm and the initial resistance measured, then stretched to 15 cm, then allowed to relax back to 10 cm in intervals of 1 cm. The resistance is measured while the fabric is clamped on the apparatus. A load-unload hysteresis curve can be plotted after this test.

2.5.3. Relaxation of the e-textile after stretching

The ability to recover from stretching is essential to maintain functionality. The garment must not creep, resulting in a permanent change in size and any permanent change in resistance should be minimised. Fabric growth after a specified extension is a standard test method for stretchable fabrics, defined by the Standard Test Methods for Stretch Properties of Fabrics Woven from Stretch Yarns (ASTM D3107) [30]. For this standard test, the fabric is held at a specified extension for a prescribed period of time. The growth is calculated from the length of the specimen prior to stretching and the length after each relaxation period at zero stress [31]. The apparatus shown in Fig. 6 is used for this test. The prescribed period of time is set as 30 min. 50% of the original clamped length of 10 cm is set as the specified extension. In Fig. 6(b), the e-textile is clamped with an initial length of 10 cm. In Fig. 6(c), it is stretched by 50% to a length of 15 cm.

The fabric length was measured immediately after the unclamping the sample(recorded as 0 in the time scale) and after intervals of 30 mins, 1 h, 3 h, 5 h, and 24 h, which are the relaxation periods defined in the standard. The resistance of the e-textiles during stretching and relaxation was also recorded.

2.5.4. Wash test

A BEKO WME7247 washing machine was used to test the resistivity change of the conductive textiles. The washing programme used was 30 ℃, 1000 rpm spin speed, with a total duration of 49 min. A plastic laundry wash ball was used with one Persil 3-in-1 Non-Bio Sensitive Laundry Washing Capsules added to every wash. The resistivity was measured after washing cycles: 0, 3, 6, 10, 15, and from cycles 20 to 100 in intervals of 10.

3. Results and discussion

3.1. Young's modulus

As shown in Fig. 7, both fabrics demonstrated good stretchability (>200%) which is sufficient for wearable applications. The stress increases with the strain during stretching. When the fabric can no longer withstand the stress, it breaks as shown by the sharp decrease in applied stress. The breaking stress is the maximum stress that can be applied to

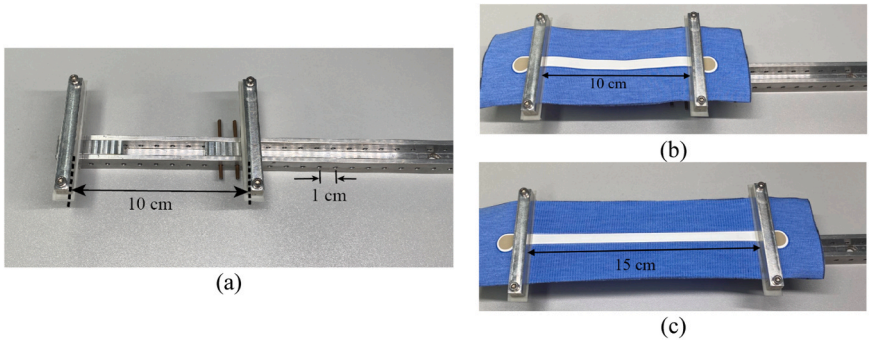

Fig. 6. (a) the stretch tool consists of two clamps and a groove. There are holes in the groove and the base of the clamps. The clamps can be fixed by two posts pushed through to holes in the groove, (b) test set-up where the blue fabric with a straight track has been clamped with a 10 cm stretchable length, (c) the fabric is stretched by 50% to 15 cm.

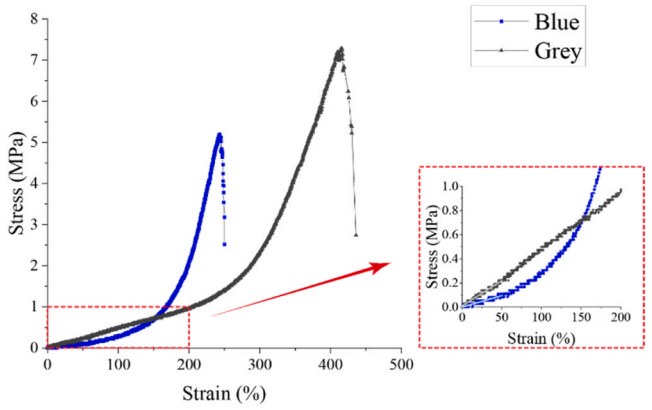

Fig. 7. The tensile stress-strain curves of the two types of fabric.

the fabric which is 5.2 MPa and an elongation of 243% for the blue fabric and 7.2 MPa and an elongation of 416% for the grey. The Young's modulus values are 0.19 Mpa for the blue fabric and 0.42 Mpa for the grey fabric for strain less than 50%, which is within the linear elastic range where deformation is reversible.

The blue fabric is composed of natural fibres (silk), semi-synthetic fibres (modal, cupro), and fully synthetic fibres (acrylic, Lycra). The use of both natural and semi-synthetic fibres in the blue fabric improves the user's comfort, as these materials are soft and can absorb moisture. However, these fibres are responsible for the blue fabric's reduced mechanical strength as compared to the grey fabric. The grey fabric is made of fully synthetic fibres (Lycra, polyester, and polyamide). The higher percentage of the elastic fibre Lycra (32%) in the grey fabric compared to the blue fabric (11%) produces higher stretchability with an elongation of 416% compared to the 243% for the blue fabric. The grey fabric provides a tighter fit in wearable applications and also requires a higher stress to generate the same level of elongation as the blue fabric at a lower strain level (less than 150%), as shown in the magnified plot in Fig. 7.

3.2. The effect of loading stretch on e-textile resistance

The change of track resistance resulting from stretch and relaxation is calculated using the equation below and the result can be plotted as a load-unload hysteresis curve for each shape and fabric, as shown in Fig. 8(a) to (d). The initial resistance of the conductive tracks for straight, sine wave, and half circle configurations ranges from 1.2 to 1.9 Ω, while horseshoe-shaped tracks exhibit an initial resistance of 2.4 to 2.5 Ω.

$$Resistance \quad change = \frac{Measured \quad resistance - Initial \quad resistance}{Initial \quad resistance}$$

Comparing Fig. 8(a)(b) with Fig. 8(c)(d), the e-textile with straight conductive tracks has the highest resistance change followed by the half circle, sine wave and horseshoe for both blue and grey fabrics. This indicates that shaped conductive tracks help to overcome the effect of stretch on resistance. For the three shaped tracks, although the horseshoe has the lowest change, the measured resistance of the horseshoe shaped tracks are similar to the sinusoidal and half circle tracks due to the initial resistance difference.

Comparing the fabric performance in Fig. 8(a) and (b), shows that the resistance change of the straight line tracks on the blue fabric is higher than on the grey fabric during stretching and relaxation up to 40% strain. For relaxation from 30% strain, the resistance change of the straight line tracks on both fabrics are similar. However, for the shaped tracks, as shown in Fig. 8(c) and (d), the resistance change of tracks on the grey textile is higher than on the blue textile.

3.3. Strain recovery of different e-textiles

The strain release rate for the four conductive tracks on both the blue and grey fabrics is shown in Figs. 9(a) and 9(b). The e-textiles with the straight conductive tracks has the slowest recovery rate followed by the horseshoe, half circle and sine wave for both blue and grey fabrics.

The e-textiles returned from 50% strain to less than 10% strain immediately after the stress was released for all the e-textiles except the blue e-textile with the straight conductive track. In particular, the grey e-textile with half circle and sine wave conductive tracks reduced to less than 4% strain immediately. Because the grey fabric is more elastic, the e-textiles with all types of conductive patterns return to around 2% strain within 5 h. Whereas the blue e-textiles still maintained more than 4% strain for the straight and horseshoe patterns and more than 2% for the half circle and sinewave patterns.

In general, the fabric growth of the grey textile is less than the blue textile for all track shapes at all recovery times. E-textiles with the sine wave track have a lower residual fabric strain for both the blue and grey textiles.

3.4. Resistance changes with 50% strain and during recovery

The resistance of the conductive tracks was measured when the e-textiles were stretched by 50% and at the strain release stage. The result is shown in Figs. 10(a) and 10(b). When the textile is stretched by 50% for 30 min, the resistance increased significantly for the straight line e-textile, by a factor of 38 times on the blue fabric and by 27 times on the grey fabric. The resistance changes for the sine wave and half circle geometries are similar on both the blue fabric (7.4 to 8.5 times) and the grey fabric (6.8 to 7 times). The horseshoe track e-textile has the lowest resistance increase, being 4.1 times larger on the blue fabric and 3.6 times larger on the grey fabric, because it has the longest track length to take up the impact of deformation during stretching. The resistance decreased rapidly after the applied force was removed from the e-textiles. The resistance change reduced to less than double the initial value for both fabrics for all conductive tracks except the straight line. Further changes after 5 h until 24 h are either zero or negligible. After 24 h the

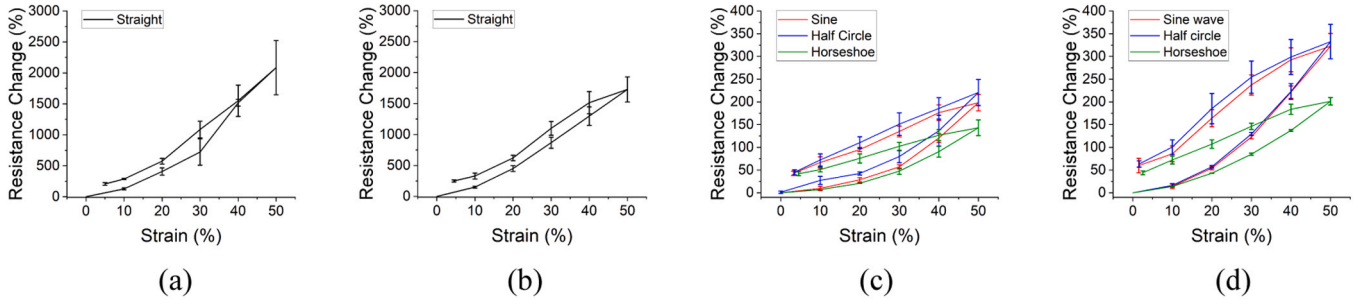

Fig. 8. (a) load-unload hysteresis curve for the straight track on the blue fabric; (b) load-unload hysteresis curve for the straight track on the grey fabric; (c) load-unload hysteresis curve for the 3 shaped tracks on the blue fabric samples; (d) load-unload hysteresis curve for the 3 shaped tracks on the grey fabric.

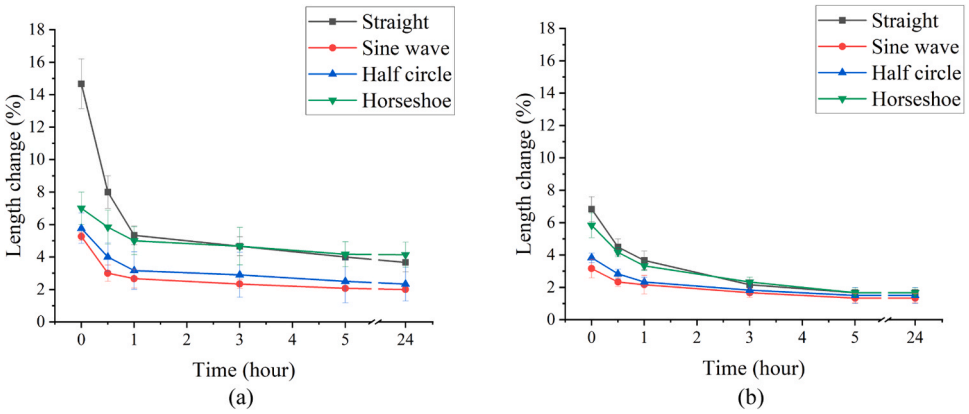

Fig. 9. (a) blue fabric strain release; (b) grey fabric strain release.

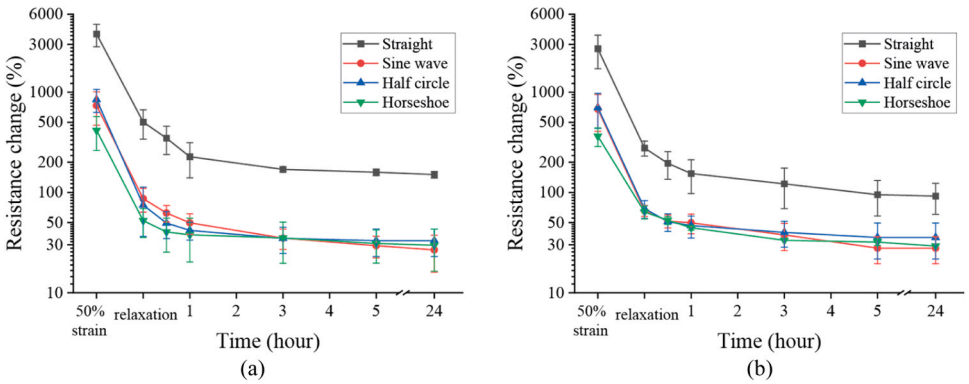

Fig. 10. (a) blue fabric resistance change with 50% strain and during recovery; (b) grey fabric resistance change with 50% strain and during recovery.

resistance change of all the fabrics except the straight line was less than 0.36 times the initial value before any extension.

3.5. Resistance changes after washing

As shown in Figs. 11(a) and 11(b), the resistance increased continuously with each wash cycle. The resistance doubled after around 50 to 70 washes for the blue textile and around 30 to 50 washes for the grey textile. After 100 wash cycles, the resistance increased by 1.20 times for the blue fabric and 1.44 times for the grey fabric. The was no significant difference in resistance change for the four structures.

3.6. Summary

The performance of the grey fabric is better than the blue fabric in the tensile, strain recovery and resistance change in stretching tests. The grey fabric provides a tighter fit in the application for which the strain is less than 150%. The length of the grey fabric recovers twice as fast as the blue fabric for all the structures investigated. The resistance of a straight line on the grey fabric is always less than three-quarters of the straight line resistance on the blue fabric. However, the blue fabric sample can be washed 20 times more than the grey fabric sample before its resistance doubled. The grey fabric is therefore chosen for the application.

Comparing the straight line, sine wave, half circle and horseshoe designs, the sine wave track has a lower material cost than the half circle or horseshoe shapes, and better performance in the load-unload

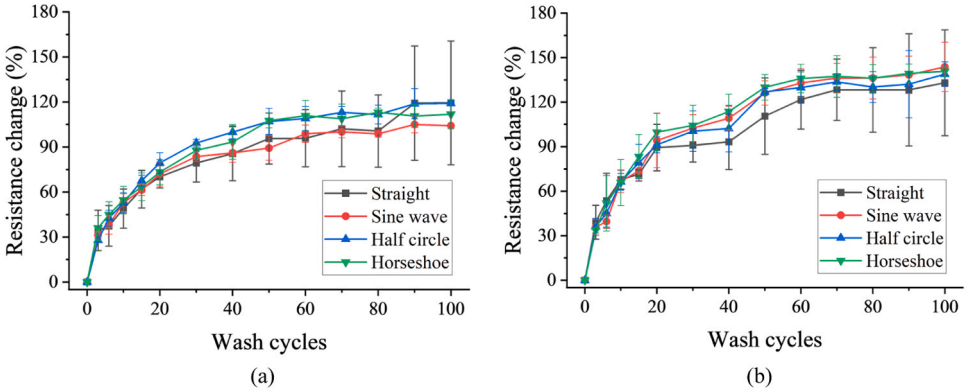

Fig. 11. (a) blue e-textile resistance change during one hundred wash cycles; (b) grey e-textile resistance change during one hundred wash cycles.

hysteresis curve compared with the straight line and half circle shapes. It also has the best performance in the strain and resistance recovery tests. The conductive tracks of the prototypes are therefore realised using the sine wave design.

4. Application in wearable electrotherapy

4.1. Fabrication of an e-textile incorporating integrated electrodes

The application is demonstrated by printing a dry electrode made from a carbon and silicone rubber layer [32] on top of a conductive layer on the textile targeting application in electrotherapy for knee joint pain relief using Transcutaneous Electrical Nerve Stimulation (TENS) technique. TENS reduces pain by stimulating sensory nerves to inhibit central transmission of pain. This is achieved by sending electrical current through the electrodes placed on the skin, typically either side of the painful area [33].

As shown in Fig. 12(a), the conductive film is printed using the sine wave structure with conductive grids at the ends to form four 4 cm by 4 cm square conductive patterns. Then, as shown in black in Figs. 12(b), 5 cm by 5 cm carbon/silicone electrodes are printed on top of the conductive patterns. The electrodes' adhesion to the fabric is strengthened by encapsulating the edges with silicone. Snap connectors are then attached to the conductive tracks at the opposite end of the electrodes to allow connection to external electronics. Finally, the areas with an exposed conductive layer are encapsulated with silicone to provide protection and electrical insulation.

4.2. Garment requirements

Aside from being close-fitting to allow for a robust connection between the skin and the electrode surfaces, the main aesthetic and functional requirements for this garment, from a pattern cutting and garment construction perspective, are user comfort, discretion, breathability, and accessibility. The comfort of the wearer is paramount, and this design needs to be able to stretch to comfortably accommodate a broad range of movements as this garment could potentially be worn while undertaking wide variety of activities, including playing sports, working at a desk, running or doing household chores, ideally without needing regular adjustment by the wearer. The garment is designed to be discreet and unobtrusive so it can be worn beneath regular clothing without adding bulk, or even under shorts without the stigma sometimes associated with wearable medical garments. Furthermore, the design is developed keeping breathability in mind – the majority of the garment is constructed from the thin grey fabric material, allowing for breathability around the knee in the event of perspiration. A thicker neoprene material is restricted to the outer perimeters of the garment where structure is required since neoprene is not breathable. Finally, accessibility is considered as the garment needs to be straightforward to don and doff, regardless of any physical limitations of the user. Hook-and-loop fasteners are chosen to accommodate users with functional limitations who might struggle with other garment closures such as snaps, buttons and zips.

4.3. Garment design

As shown in Fig. 13(a), the garment has been designed as a wrap-around sleeve, comprised of two panels – a central grey e-textile surrounded on three sides by a black neoprene panel. The thicker black neoprene material, consisting of a 0.8 mm perforated neoprene layer sandwiched between two layers of hook and loop receptive fabric, provides support and structure to the garment. The neoprene panel is pattern cut with two darts on the lower edge, enabling a contoured effect around the curves of the calf, as well as with shaping provided by lengthening the rise of the neoprene panel where it joins with the grey fabric to provide shaping around the upper knee and thigh. Creating shaping in this way allows the central panel to lie flat for electrode and circuit lamination prior to assembly.

Five hook-and-loop tabs were stitched to the garment at points A.1, A.2, A.3 and A.4 on the neoprene material and point B.1 on the grey material as shown in Fig. 13(a). As the neoprene is hook-and-loop receptive; the tabs can be adjusted to adapt to diverse body shapes. The hook-and-loop tabs at points A.1 and A.2 wrap around the back of the leg and attach to regions on the upper inner thigh and upper front thigh. The tabs at points A.3 and A.4 wrap around the lower leg and attach to the neoprene below the knee at the calf. Point B.1 attaches to the neoprene at the inner knee. The portion of the neoprene panel that wraps around the knee has a cut-out region, allowing for greater flexibility around the knee joint while also providing structure and rigidity to the garment.

The garment was stitched together using zig-zag stitches which tolerate a high level of stretching without breaking, and the darts on the lower edge of the neoprene panel were sewn together using abutted seams – sewn edge-to-edge with no overlap, thus reducing bulk and the potential for skin irritation. Fig. 13(b) shows the finished garment. Figs. 13(c) and 13(d) are the front view and side view of the garment on a mannequin's leg.

5. Conclusions

This research has developed a method to fabricate stretchable e-textiles made of laminated conductive film and silicone/carbon electrodes. The Young's modulus of the grey fabric is higher than that of the blue fabric when the strain is less than 130%. This prevents the e-textile being over stretched and provides a faster recovery when the strain is released, which is essential to maintaining good contact between the e-textile and the skin, especially during movement. A sinusoidal track provides the fastest strain recovery from stretching compared with a straight line, half circle and horseshoe shapes. Therefore, it is recommended for applications where e-textiles require good elasticity. The horseshoe e-textile demonstrates the best conductivity of the track geometries when the e-textile is stretched by the same percentage. This makes it more suitable for applications where resistivity change needs to be minimised. After stretchability tests, all e-textiles still survived 100 wash cycles with a maximum resistance increase of 1.44 times. This research also results in the development of a wraparound sleeve for wearable electrotherapy applications based on the above e-textile. The

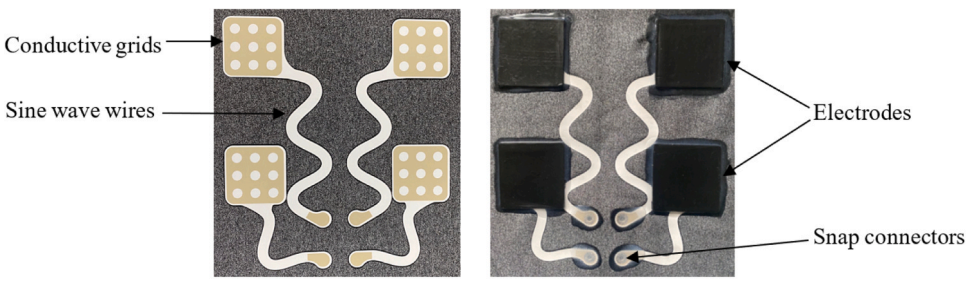

Fig. 12. (a) e-textile with laminated conductive film; (b) e-textile with a black carbon layer, encapsulated layer and snap buttons.

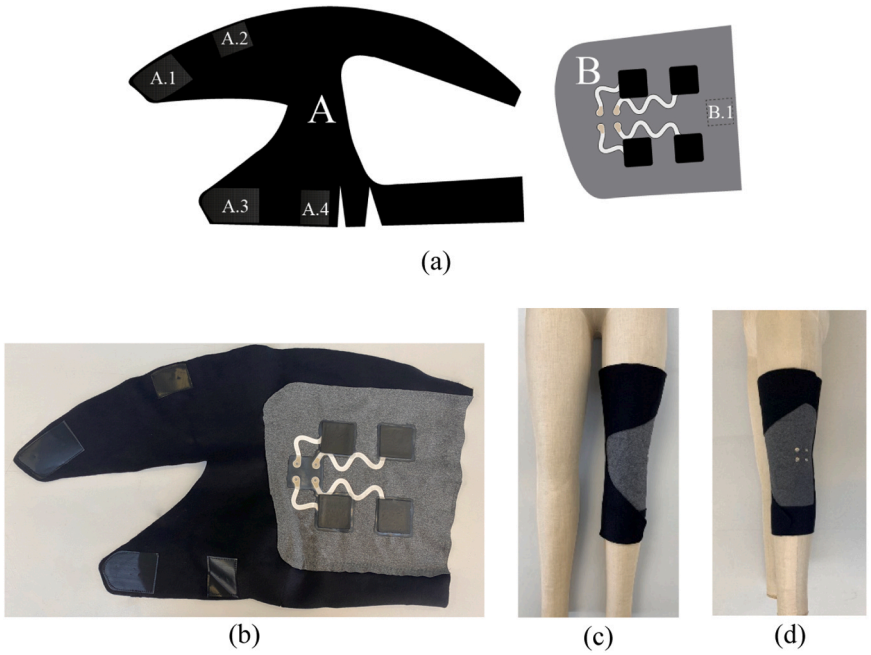

Fig. 13. (a) the garment is formed by assembling two panels (A and B); (b) the finished garment; (c) front view of the garment on a mannequin's leg; (d) side view of the garment on a mannequin's leg. The snap is located on the outside of the knee.

grey fabric and sinusoidal tracks are chosen to form the electrode textile. A sleeve with optimized usability is achieved by neoprene fabric panels which were pattern cut with darts converted to seams at each junction, enabling a contoured effect around the curves of the knee.

CRediT authorship contribution statement

Yang Kai: Conceptualization, Funding acquisition, Resources, Supervision, Writing – review & editing. **Tudor John:** Validation, Writing – review & editing. **Beeby Steve:** Supervision, Writing – review & editing. **Wescott Alison:** Investigation. **Lake-Thompson Gillian:** Investigation, Writing – original draft. **Liu Meijing:** Conceptualization, Data curation, Formal analysis, Investigation, Methodology, Visualization, Writing – original draft.

Declaration of Competing Interest

The authors declare that they have no known competing financial interests or personal relationships that could have appeared to influence the work reported in this paper.

Data availability

The data supporting this study's results are available within the article.

Acknowledgements

The authors would like to acknowledge funding from the EPSRC under grant number EP/S001654/1 and MRC under grant number MR/W029421/1. The authors also thank the Best Pacific Limited (Dongguan, China) for supplying the fabrics. The work of Steve Beeby was supported by the RAEng under the Chairs in Emerging Technologies Scheme.

References

[1] A. Komolafe, B. Zaghari, R. Torah, A.S. Weddell, H. Khanbareh, Z.M. Tsikriteas, M. Vousden, M. Wagih, U.T. Jurado, J. Shi, S. Yong, S. Arumugam, Y. Li, K. Yang, G. Savelli, N.M. White, S. Beeby, E-textile technology review–from materials to application, IEEE Access vol. 9 (2021) 97152–97179, https://doi.org/10.1109/ACCESS.2021.3094303.

[2] S. Yong, M. Liu, A. Komolafe, J. Tudor, K. Yang, Development of a screen-printable carbon paste to achieve washable conductive textiles, Textiles vol. 1 (3) (. 2021) 419–432, https://doi.org/10.3390/textiles1030022.

[3] V. Sanchez, C.J. Payne, D.J. Preston, J.T. Alvarez, J.C. Weaver, A.T. Atalay, M. Boyvat, D.M. Vogt, R.J. Wood, G.M. Whitesides, C.J. Walsh, Smart thermally actuating textiles, Adv. Mater. Technol. vol. 5 (8) (. 2020), https://doi.org/10.1002/admt.202000383.

[4] J. Zhong, H. Zhou, Y. Liu, X. Cheng, L. Cai, W. Zhu, L. Liu, Integrated design of physiological multi-parameter sensors on a smart garment by ultra-elastic E-textile, J. Mech. Med Biol. vol. 21 (09) (. 2021), https://doi.org/10.1142/S0219519421400376.

[5] A. Komolafe, R. Torah, Y. Wei, H. Nunes-Matos, M. Li, D. Hardy, T. Dias, M. Tudor, S. Beeby, Integrating flexible filament circuits for E-textile applications, Adv. Mater. Technol. vol. 4 (7) (. 2019), https://doi.org/10.1002/admt.201900176.

[6] M. Wagih, G.S. Hilton, A.S. Weddell, S. Beeby, Dual-band dual-mode textile antenna/rectenna for simultaneous wireless information and power transfer (SWIPT), IEEE Trans. Antennas Propag. vol. 69 (10) (. 2021) 6322–6332, https://doi.org/10.1109/TAP.2021.3070230.

[7] M.E. Tavares Sousa, H.D. de Andrade, J.L. da Silva Paiva, F. de Assis Brito Filho, I. Barros Tavares da Silva, M. Silva de Aquino, M. Vieira de Melo, Development of a wireless communication prototype based on e-textile concept for application in healthcare monitoring of patients subject to sacral pressure injuries, Res. Biomed. Eng. vol. 37 (4) (. 2021) 673–685, https://doi.org/10.1007/s42600-021-00180-1.

[8] Healthcare, Wearable Medical Device Market Size." Accessed: Sep. 04, 2023. [Online]. Available: https://www.grandviewresearch.com/industry-analysis/wearable-medical-devices-market.

[9] G. Paul, R. Torah, S. Beeby, J. Tudor, The development of screen printed conductive networks on textiles for biopotential monitoring applications, Sens Actuators A Phys. vol. 206 (. 2014) 35–41, https://doi.org/10.1016/j.sna.2013.11.026.

[10] T. Ward, N. Grabham, C. Freeman, Y. Wei, A.-M. Hughes, C. Power, J. Tudor, K. Yang, Multichannel biphasic muscle stimulation system for post stroke rehabilitation, Electron. (Basel) vol. 9 (7) (. 2020) 1156, https://doi.org/10.3390/electronics9071156.

[11] M. Liu, T. Ward, D. Young, H. Matos, Y. Wei, J. Adams, K. Yang, Electronic textiles based wearable electrotherapy for pain relief, Sens Actuators A Phys. vol. 303 (2020) 111701, https://doi.org/10.1016/j.sna.2019.111701.

[12] L. Hernandez, Smart Sock Feasibility Study. in E-Textiles 2022, MDPI, Basel Switzerland, . 2023, p. 11, https://doi.org/10.3390/engproc2023030011.

[13] H. Ryu, S. Park, J.-J. Park, J. Bae, A knitted glove sensing system with compression strain for finger movements, Smart Mater. Struct. vol. 27 (5) (2018) 055016, https://doi.org/10.1088/1361-665X/aab7cc.

[14] K. Fobelets, G. Hammour, K. Thielemans, Knitted ECG electrodes in relaxed fitting garments, IEEE Sens J. vol. 23 (5) (. 2023) 5263–5269, https://doi.org/10.1109/JSEN.2023.3236723.

[15] S. Ke, Q. Xue, C. Pang, P. Guo, W. Yao, H. Zhu, W. Wu, Printing the ultra-long Ag nanowires inks onto the flexible textile substrate for stretchable electronics, Nanomaterials vol. 9 (5) (2019) 686, https://doi.org/10.3390/nano9050686.

[16] M. Jose, M. Lemmens, S. Bormans, R. Thoelen, W. Deferme, Fully printed, stretchable and wearable bioimpedance sensor on textiles for tomography, Flex. Print. Electron. vol. 6 (1) (. 2021) 015010, https://doi.org/10.1088/2058-8585/abe51b.

[17] M. Liu, S. Arumugam, Y. Li, S. Yong, N. White, K. Yang, S. Beeby, Printable Piezoresistive Carbon Formulation for Stretch and Flex Sensors in E-Textile Applications. IEEE International Conference on Flexible and Printable Sensors and Systems (FLEPS), IEEE,, . 2019, pp. 1–3, https://doi.org/10.1109/FLEPS.2019.8792236.

[18] Y. Lin, X. Chen, Q. Lu, J. Wang, C. Ding, F. Liu, D. Kong, W. Yuan, W. Su, Z. Cui, Thermally laminated lighting textile for wearable displays with high durability, ACS Appl. Mater. Interfaces vol. 15 (4) (. 2023) 5931–5941, https://doi.org/10.1021/acsami.2c20681.

[19] A. Hermann, J. Ostarhild, Y. Mirabito, N. Bauer, V. Senner, Stretchable Piezoresistive vs. Capacitive Silicon Sensors Integrated into Ski Base Layer Pants for Measuring the Knee Flexion Angle, Sports Eng. vol. 23 (1) (2020), https://doi.org/10.1007/s12283-020-00336-9.

[20] B. Abtahi, M. Warncke, H. Winger, C. Sachse, E. Häntzsche, A. Nocke, C. Cherif, Novel Strain Sensor in Weft-Knitted Textile for Triggering of Functional Electrical Stimulation. in E-Textiles 2022, MDPI, Basel Switzerland, . 2023, p. 13, https://doi.org/10.3390/engproc2023030013.

[21] Geo Knight DK20S 16×20 Digital Swing Away Heat Press." Accessed: Jan. 06, 2024. [Online]. Available: https://www.rasmartmachinery.co.uk/product/geo-knight-dk20s-16×20-digital-swing-away-heat-press/.

[22] M. Catchpole, E-textile seam crossing with screen printed circuits and anisotropic conductive film. in International Conference on the Challenges, Opportunities, Innovations and Applications in Electronic Textiles, MDPI, Basel Switzerland, . 2019, p. 16, https://doi.org/10.3390/proceedings2019032016.

[23] M. Liu, T. Ward, O. Keim, Y. Yin, M. Tudor, and K. Yang, Smart Textile with Integrated Functional Electrical Stimulation and Movement Sensor for Hand Exercise, in *Annual Conference of the International Functional Electrical Stimulation Society (IFESS): RehabWeek 2022*, Rotterdam, 2022. doi: 10.1111/aor.14408.

[24] Healthcare World, Tens Lead Wires With Snap Connection & female Tens Plug Connection One Pair." Accessed: Sep. 04, 2023. [Online]. Available: https://www.hcwhealth.com/tens-lead-wires-with-snap-connection-female-tens-plug-connection-one-pair.

[25] Best from Japan, Snap button." Accessed: Sep. 04, 2023. [Online]. Available: http://www.bestfromjapan.com/faq/topic.cfm?topicid=206.

[26] Y. Huang, Y. Ding, J. Bian, Y. Su, J. Zhou, Y. Duan, Z. Yin, Hyper-stretchable self-powered sensors based on electrohydrodynamically printed, self-similar piezoelectric nano/microfibers, Nano Energy vol. 40 (. 2017) 432–439, https://doi.org/10.1016/j.nanoen.2017.07.048.

[27] K. Kim, K. Jung, S. Jung, Design and fabrication of screen-printed silver circuits for stretchable electronics, Micro Eng. vol. 120 (2014) 216–220, https://doi.org/10.1016/j.mee.2013.07.003.

[28] A.A. Norhidayah, A.A. Saad, M.F.M. Sharif, F.C. Ani, M.Y.T. Ali, M.S. Ibrahim, Z. Ahmad, Stress analysis of a stretchable electronic circuit, Procedia Eng. vol. 184 (2017) 625–630, https://doi.org/10.1016/j.proeng.2017.04.127.

[29] N. Wei, K. Pan, H. Lin, R. Chen, B. Guo, Optimistic Design of Freestanding Horseshoe Metal Interconnects For Stretchable Electronic Circuits. 15th International Conference on Electronic Packaging Technology, IEEE, 2014, pp. 1526–1529, https://doi.org/10.1109/ICEPT.2014.6922944.

[30] ASTM D3107–07:2015. Standard Test Methods for Stretch Properties of Fabrics Woven From Stretch Yarns.

[31] A. Khalil and P. Těšinová, Elastic Recovery of Full Plaited Knitted Fabric, in *21st World Textile Conference, AUTEX 2022 Conference Proceedings*, Lodz, Poland, Jun. 2022. Accessed: Jun. 27, 2023. [Online]. Available: https://repozytorium.p.lodz.pl/handle/11652/4514.

[32] M. Liu, S. Beeby, K. Yang, Electrode for Wearable Electrotherapy. in International Conference on the Challenges, Opportunities, Innovations and Applications in Electronic Textiles, MDPI, Basel Switzerland, . 2019, p. 5, https://doi.org/10.3390/proceedings2019032005.

[33] TENS (transcutaneous electrical nerve stimulation). Accessed: Jan. 12, 2024. [Online]. Available: https://www.nhs.uk/conditions/transcutaneous-electrical-nerve-stimulation-tens.

Meijing Liu. is currently a final year PhD student in Electronic and Electrical Engineering at Smart Electronic Materials & Systems group, University of Southampton. She is also a research fellow at E-textile Innovation Lab, Winchester School of Art. She obtained a M.S. degree in Microelectromechanical Systems (MEMS), from University of Southampton, UK in 2018 and a B.S. degree in Microelectronics Science and Engineering, from Guilin University of Electronic Technology, China in 2017. Her research focuses on advanced E-textiles for healthcare applications.